Contrasting the Charge Carrier Mobility of Isotactic, Syndiotactic, and Atactic Poly((*N*-carbazolylethylthio)propyl methacrylate)

Sanket Samal, Alexander Schmitt, and Barry C. Thompson*

Department of Chemistry, Loker Hydrocarbon Research Institute, University of Southern California, Los Angeles, California 90089-1661, United States.

ABSTRACT: Isotactic non-conjugated pendant electroactive polymers (NCPEPs) have recently shown potential to achieve comparable charge carrier mobilities with conjugated polymers. Here we report the broader influence of tacticity in NCPEPs, using Poly((*N*-carbazolylethylthio)propyl methacrylate) (PCzETPMA) as a model polymer. We utilized the thiol-ene reaction as an efficient post-polymerization functionalization method to achieve pendant polymers with high isotacticity and syndiotacticity. We found that a stereoregular isotactic polymer showed ~100 times increased hole mobility (μ_h) as compared to both atactic and low molecular weight syndiotactic PCzETPMA, achieving μ_h of 2.19 x 10^{-4} cm^2 V^{-1} s^{-1} after annealing at 120 °C. High molecular weight syndiotactic PCzETPMA gave ~10 times higher μ_h than its atactic counterpart, comparable to isotactic PCzETPMA after annealing at 150 °C. Importantly, high molecular weight syndiotactic PCzEPTMA showed a dramatic increase in μ_h to 1.82 x 10^{-3} cm^2 V^{-1} s^{-1} when measured after annealing at 210 °C, which surpassed the well-known conjugated polymer poly(3-hexylthiophene) (P3HT) (μ_h = 4.51 x 10^{-4} cm^2 V^{-1} s^{-1}). MD simulations indicated short range $\pi - \pi$ stacked ordering in the case of stereoregular isotactic and syndiotactic polymers. This work is the first report of charge carrier mobilities in syndiotactic NCPEPs and demonstrates that the tacticity, annealing conditions, and molecular weight of NCPEPs can strongly affect μ_h.

With the development of novel manufacturing technologies, conjugated polymers (CP) are emerging as viable materials for many optoelectronic applications, such as organic photovoltaics (OPVs),[1–3] organic field-effect transistors (OFETs),[4,5] organic light-emitting diodes (OLEDs),[6,7] batteries,[8–10] and bioelectronics[11,12] due to their numerous advantages over inorganic analogs. Among various benefits of CPs such as lightweight, low cost, low toxicity, and easy processibility, the high charge carrier mobilities of CPs plays a crucial role in the fabrication of high-performance devices such as OPVs and OFETs.[13]

Despite outstanding performance in optoelectronic applications, CPs nonetheless are limited by several challenges.[14] While approaches have recently been developed to overcome some of these challenges;[15–17] notably, CPs still lack effective synthetic methods to make narrow dispersity and high molecular weight polymers, which are crucial for the fabrication of efficient optoelectronic devices[18] and the development of advanced architectures such as block copolymers.[19,20] Poor environmental stability and restricted mechanical properties are also limitations of CPs.[21,22]

Recently non-conjugated electroactive polymers have been explored in many fields as an alternative for CPs.[23,24] Specifically, non-conjugated pendant electroactive polymers (NCPEPs), which are non-conjugated polymers containing electroactive units in the side chain, possess enormous potential. Such polymers offer access to the broad range of controlled polymerization techniques of non-conjugated polymers that promise access to highly tailored structures with diverse architectures.[25] With NCPEPs, in analogy to side-chain liquid crystal polymers,[26,27] optoelectronic properties are strongly influenced by the structure of the polymer backbone, pendant group, spacer (length and identity), and stereoregularity (Figure **1**).

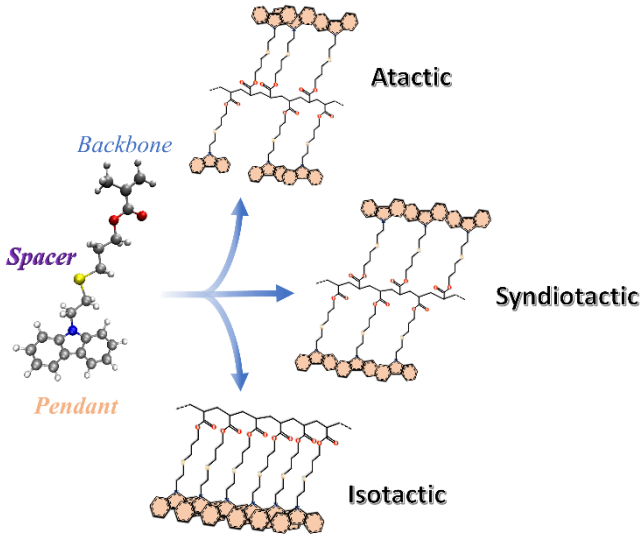

Figure 1. Structural features impacting properties in NCPEPs: Backbone structure, spacer length, pendant group and stereoregularity.

In our recent study, we demonstrated the impact of isotacticity relative to atactic polymers, where we found that hole mobility (μ_h) of NCPEPs increases proportionally to the increasing isotacticity, achieving μ_h ~100 times higher than atactic analogs.[28] We further showed the effect of the spacer length on the μ_h of NCPEPs, where we found that a six carbon alkyl spacer is the optimum flexible spacer length to achieve high μ_h in isotactic NCPEPs using highly isotactic poly(*N*-carbazolylalkyl acrylates) as our model system.[29]

Although NCPEPs promise to overcome limitations of CPs, and examples exhibiting higher charge carrier mobilities than CPs have

been reported,[30,31] NCPEPs are generally found to have charge carrier mobilities several orders of magnitude lower than CPs.[32] Taking inspiration from the work of Uryu et al.,[33] who showed that highly isotactic (*m* = ~97%) poly(2-*N*-carbazolylethyl acrylate) (PCzEA) had a μ_h of 1.7 x 10^{-5} cm^2 V^{-1} s^{-1}; being six times higher than the atactic counterpart, we have recently showed clear evidence for the correlation of stereoregularity in PCzEA and μ_h. We found that μ_h increased from 2.11 x 10^{-6} cm^2 V^{-1} s^{-1} to 4.68 x 10^{-5} cm^2 V^{-1} s^{-1} in unannealed samples as the dyad isotacticity increased from *m* = ~45% to *m* = ~95%, and the μ_h is further increased to 2.74 x 10^{-4} cm^2 V^{-1} s^{-1} with thermal annealing of the ~95% isotactic sample, which is as par with most of the well-known CPs such as poly(3-hexylthiophene) (P3HT).[34]

However, our study of the effect of stereoregularity on the μ_h of NCPEPs was limited to isotactic PCzEA, and further work done by Ozaki et al.,[35] on poly(N-vinylcarbazole) (PVK), was also limited to the isotactic polymer. For designing optimized NCPEPs proper understanding of the structure-function relationships is required. As such, here we further investigate the effect of stereoregularity on the μ_h of NCPEPs by comparing isotactic, syndiotactic and atactic polymers, keeping the pendant group, spacer length, and polymer backbone constant.

We report a novel methodology for synthesis of a family of poly((N-carbazolylethylthio)propyl methacrylate) (PCzETPMA) polymers with different tacticity including isotactic PCzETPMA (*mm* = ~85%), syndiotactic PCzETPMA (*rr* = ~80%) with two different molecular weights, and an atactic PCzETPMA. Using the previously determined optimal spacer length of six atoms,[29] we find that both isotactic and atactic PCzETPMA give comparable results to our previously reported isotactic and atactic NCPEPs. Interestingly the low molecular weight syndiotactic PCzETPMA gave similar μ_h to the atactic counterpart while the high molecular weight syndiotactic PCzETPMA gave comparable μ_h to the isotactic counterpart. However, higher temperature annealing of the high molecular weight syndiotactic polymer resulted in μ_h ten times higher than isotactic PCzETPMA.

Consistent with our observation for acrylate polymers, anionic polymerization gave the best control over tacticity, and hence anionic polymerization was preferred for this study. To avoid the limitations of anionic polymerization, we used a post-polymerization route using the thiol-ene reaction, which has been broadly used for post-polymerization functionalization.[36,37] We used allyl methacrylate which has proven effective in yielding both isotactic and syndiotactic polymers via anionic polymerization[38,39] and the allyl group is amenable to post-polymerization functionalization.[40,41]

Scheme 1. Synthesis of (a) Pendant group, (b) PAMA polymers, and (c) PCzETPMA polymers.

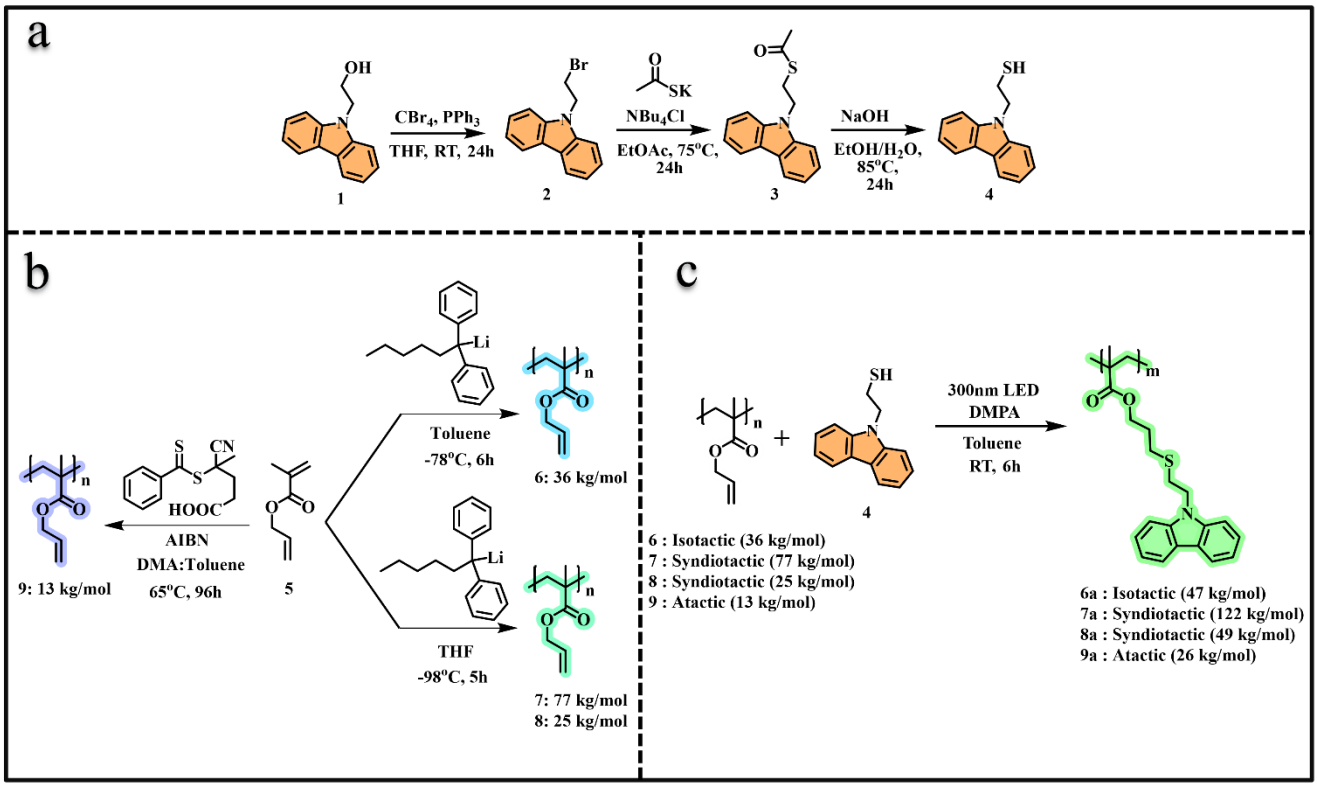

N-carbazolylethanethiol chosen as the electroactive pendant for the thiol-ene reaction as to achieve the optimized spacer length and have the same pendant unit as our previous studies.[28,29] Synthesis of *N*-carbazolylethanethiol (**4**) is depicted in Scheme **1a**. To achieve the desired polymers (**6** – **9**), allyl methacrylate was polymerized under different conditions as depicted in Scheme **1b**, with molecular weight and tacticity data shown in Table **1**. To synthesize the isotactic polymer (**6**), allyl methacrylate was reacted using freshly prepared diphenylhexyllithium (DPHL) as the initiator in toluene, while syndiotactic polymers (**7** and **8**) were obtained using DPHL as the initiator but using THF as solvent. Similar approaches for allyl methacrylate were reported in the literature.[39] The difference in stereoregularity using different solvents is based on solvation of the lithium cation. In the case of toluene, the lithium cation is not solvated and hence binds with the terminal and penultimate carbonyl oxygens yielding an isotactic polymer,[43] while in the case of THF, the

lithium cations are fully solvated and hence cannot bind carbonyl oxygens giving syndiotactic polymer.[44,45] Finally to achieve the atactic polymer (**9**), we chose reversible addition-fragmentation chain-transfer (RAFT) polymerization since it yielded a reproducible level of tacticty.[46] Triad and pentad tacticity for all the polymers were calculated from ^{1}H and ^{13}C NMR respectively (Table **1** and Supporting information) and are referenced from PMMA NMR peak shifts.[47] Under the described conditions atactic (**9**) (*rr* = ~50%), isotactic (**6**) (*mm* = ~85%), and syndiotactic (**8**) (*rr* = ~80%) PAMA samples were achieved with M_n values of 12.6, 36.4, and 24.9 kg/mol, respectively. Increasing the monomer concentration from 5 mmol to 10 mmol led to a significant increase in M_n with anionic polymerization in THF to give polymer **7** (*rr* = ~80%) of 77.3 kg/mol. The effect of monomer concentration on the molecular weight of the PMMA is well studied showning similar results in the literature.[38] High molecular weight isotactic and atactic polymers were not targeted because of the lower solubility in these cases.

Table 1. Polymer Yields/Conversions, Molecular Weights, *Đ*, Triad and pentad tacticity and SCLC mobilities for the family of PCzETPMA polymers.

Polymer	Yield[a]/ Conversion[b] (%)	M_n (kg/mol)[c]	*Đ*	Triad Tacticity[d] (%)	Pentad Tacticity[e] (%)	μ_h ($cm^2V^{-1}s^{-1}$)[f,j] Unannealed	μ_h ($cm^2V^{-1}s^{-1}$)[g,j] Annealed at 120˚C	μ_h ($cm^2V^{-1}s^{-1}$)[h,j] Annealed at 150˚C	μ_h ($cm^2V^{-1}s^{-1}$)[i,j] Annealed at 210˚C
6	75[a]	36.4	1.4	85 (*mm*)	80 (*mmmm*)	-	-	-	-
7	90[a]	77.3	1.2	80 (*rr*)	70 (*rrrr*)	-	-	-	-
8	85[a]	24.9	1.4	80 (*rr*)	70 (*rrrr*)	-	-	-	-
9	55[a]	12.6	1.4	50 (*rr*)	50 (*rrrr*)	-	-	-	-
6a	>99[b]	46.5	2.3	85 (*mm*)	80 (*mmmm*)	$(6.0\pm0.75)\times10^{-5}$	$(2.19\pm0.22)\times10^{-4}$	$(1.6\pm0.95)\times10^{-4}$	$(1.47\pm0.55)\times10^{-4}$
7a	>99[b]	122.1	1.2	80 (*rr*)	70 (*rrrr*)	$(2.1\pm0.60)\times10^{-6}$	$(1.1\pm0.28)\times10^{-4}$	$(1.37\pm0.52)\times10^{-4}$	$(1.82\pm0.48)\times10^{-3}$
8a	>99[b]	49.4	1.5	80 (*rr*)	70 (*rrrr*)	$(2.59\pm0.34)\times10^{-7}$	$(2.23\pm0.41)\times10^{-8}$	$(3.22\pm0.66)\times10^{-8}$	$(9.81\pm1.1)\times10^{-7}$
9a	>99[b]	26.1	1.6	50 (*rr*)	50 (*rrrr*)	$(1.17\pm0.62)\times10^{-7}$	$(4.03\pm0.44)\times10^{-8}$	$(3.79\pm0.32)\times10^{-8}$	$(4.37\pm0.70)\times10^{-7}$

[a]Polymerization yield, [b]Thiol-ene conversion, determined by ^{1}H NMR. [c]Determined by SEC with polystyrene standards and TCB eluent. [d]Determined from ^{1}H NMR. [e]Determined from ^{13}C NMR. [f]Measured from neat, as-cast polymer films. [g]Measured from polymer films after 30 min annealing at 120 ˚C. [h]Measured from polymer films after 30 min annealing at 150 ˚C. [i]Measured from polymer films after 30 min annealing at 210 ˚C. [j]Data represents an average of at-least 20 pixels.

Polymers **6** – **9** were then subjected to a photochemical thiol-ene reaction with compound **4**, using 2,2-dimethoxy-2-phenylacetophenone (DMPA) as photoinitiator and a 300nm LED as light source. The photochemical thiol-ene route gave >99% conversion and was highly selective for the anti-Markonikov product as compared to other reported reaction conditions.[48] Synthesis of polymers **6a** – **9a** is depicted in Scheme **1a**, and the method is adapted from literature with slight variation.[49] This thiol-ene post-polymerization functionalization technique gives us a pathway to achieve new functional NCPEPs with suitable tacticity and molecular weights with minimal to no defects. Both syndiotactic polymers (**7a** – **8a**) are readily soluble in chloroform up to 50 mg/ml at room temperature. In contrast, the atactic (**9a**) and the isotactic polymers (**6a**) were only soluble at 60 ˚C in chloroform at 10 mg/ml.

The space charge limited current (SCLC) technique was used to measure the μ_h of polymer thin films with and without annealing (Table **1** and Figure **2**). All the SCLC measurements were repeated three times, and the data reported are an average of at-least 20 pixels. The annealing temperatures were not extensively optimized and annealing above 210 ˚C was avoided as the atactic polymer (**9a**) started to lose more than 5 % of mass above 220 ˚C as observed in TGA (supporting information). All the polymers were spin-coated from $CHCl_3$ to yield films with thickness of 50 – 65 nm. For the atactic polymer **9a**, annealed and unannealed samples showed μ_h in the range of 10^{-7}–10^{-8} $cm^2V^{-1}s^{-1}$. For the isotactic polymer **6a**, the unannealed sample gave μ_h of 6.0×10^{-5} $cm^2 V^{-1} s^{-1}$ which increased to 2.19×10^{-4} $cm^2 V^{-1} s^{-1}$ when the film is annealed at 120 ˚C for 30 mins. With annealing at higher temperatures, μ_h decreased to 1.47×10^{-4} $cm^2 V^{-1} s^{-1}$ when annealed at 210 ˚C for 30 mins. The μ_h at the 120 ˚C annealing condition is on par with the unannealed μ_h of well-known conjugated polymer poly(3-hexylthiophene) (P3HT)[50] and is similar to our previous NCPEP studies confirming that high μ_h can be achieved with isotactic NCPEPs.

Interestingly the two syndiotactic polymers gave significantly different results. For the low molecular weight syndiotactic polymer **8a**, unannealed films gave μ_h of 2.59×10^{-7} $cm^2 V^{-1} s^{-1}$, which is two orders of magnitude lower than unannealed isotactic polymer **6a** and nearly identical with the unannealed atactic polymer **9a**. On annealing of **8a**, μ_h decreased to 2.23×10^{-8} $cm^2 V^{-1} s^{-1}$ when annealed at 120 ˚C for 30 mins. However, with annealing at 210 ˚C for 30 mins **8a** showed an increased value with a maximum 9.81×10^{-7} $cm^2 V^{-1} s^{-1}$ thus showing a similar trend to the atactic polymer (Figure **2**). For the low molecular weight syndiotactic polymer **8a**, even after annealing μ_h is still two orders of magnitude lower than its isotactic counterpart which has comparable molecular weight (49.4 and 46.5 kg/mol, respectively).

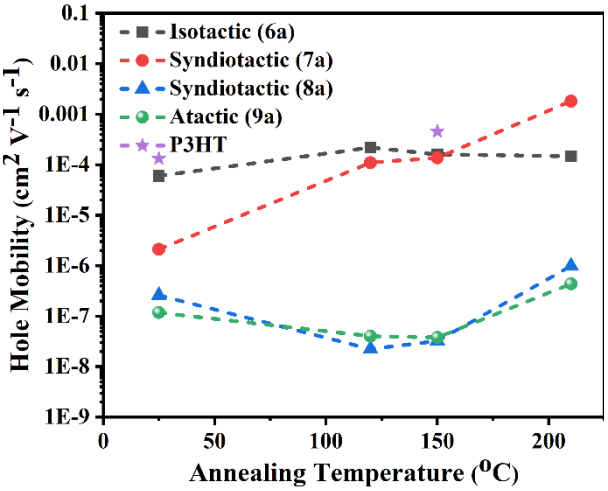

Figure 2. Effect of annealing on hole mobility of PCzETPMA polymers with different tacticity.

In contrast, with the high molecular weight syndiotactic polymer **7a**, even the unannealed sample gave μ_h of 2.1 x 10^{-6} $cm^2 V^{-1} s^{-1}$. The μ_h of polymer **7a** is observed to increase to 1.37 x 10^{-4} $cm^2 V^{-1} s^{-1}$ upon annealing at 120 °C for 30 mins. Upon annealing at 210 °C for 30 mins the μ_h reached the increased value of 1.82 x 10^{-3} $cm^2 V^{-1} s^{-1}$, surpassing annealed P3HT and isotactic polymer **6a** by an order of magnitude. This result is unprecedented and shows a clear effect of molecular weight on the μ_h of the syndiotactic polymer.

For further comprehension of the mobility – tacticity relationships, we investigated several characterization techniques. First, we measured thin film UV–vis absorption, where we saw little to no difference between all the polymers **6a** – **9a** for both annealed and unannealed samples (supporting information). For all films, characteristic carbazole $\pi - \pi^*$ transitions (~295 nm) and $n - \pi^*$ transitions (~330 and 344 nm) were observed. The HOMO levels of all the polymer were also found to be similar as measured by cyclic voltammetry (CV) showing no effect of tacticity (5.62 – 5.69 eV) (supporting information). The above-mentioned HOMO value is 0.2 eV higher than previously reported PCzXA values as in this case the HOMO is delocalized to the nearby S atom (Figure **3a**).

In contrast to UV–vis absorption and cyclic voltammetry, Photoluminescence (PL) spectra gave some structural insight (Fig **3b** and **3c**). For the unannealed films (Fig **3b**), we see characteristic 0 – 0 transitions at 350 nm with a sharper vibronic band at 370 nm, which are typical for carbazole and are similar to our previous studies. Peaks around 405 to 430 nm corresponding to excimer emission are not prominent.[51] Both low molecular weight syndiotactic polymer (**8a**) and atactic polymer (**9a**) show lower PL intensity than isotactic (**6a**) and high molecular weight syndiotactic polymer (**7a**), implying more aggregation in polymers **8a** and **9a** for unannealed films. Similar spectral shapes are observed in the case of annealed thin films (Fig **3c**). For the atactic polymer **9a**, there is no effect of annealing giving the same PL intensity for both unannealed and annealed thin films. Interestingly, for the polymers **6a** and **7a**, the PL intensity is strongly diminished, suggesting aggregation based PL quenching, and thus providing some evidence towards enhanced $\pi - \pi$ stacking on annealing with the isotactic and high molecular weight syndiotactic polymers. On the other hand, for polymer **8a**, on annealing the PL intensity is increased and the excimer peaks are further diminished, suggesting reduced $\pi - \pi$ stacking.

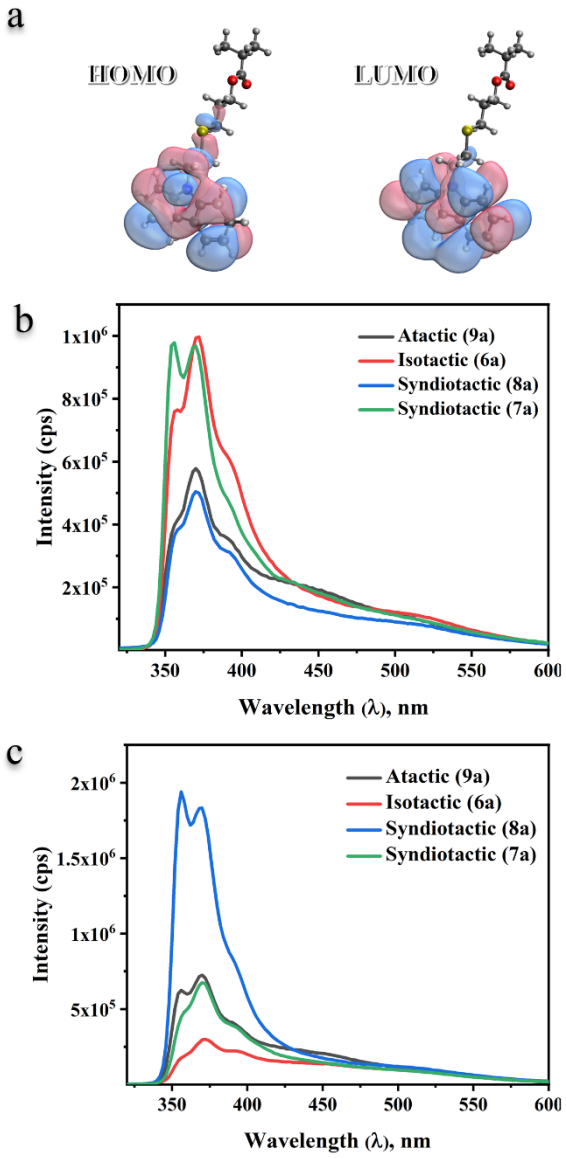

Figure 3. **(a)** HOMO and LUMO of PCzETPMA repeating unit. **(b)** PL spectra of PCzETPMA polymers as-cast films. **(c)** PL spectra of PCzETPMA polymers films after annealing at 210 °C for 30 mins.

To study the morphology more precisely, the thin films were examined by grazing incidence X-ray diffraction (GIXRD); however, no peaks were observed for polymers **6a** – **9a** with or without annealing (supporting information), which is in agreement with our previous studies indicating the polymers are largely amorphous. The findings from GIXRD are also consistent with DSC where no prominent peaks were observed (supporting information) expect for a small endothermic peak around 65 °C in the case of polymer **7a** which was only observed in the first cycle. While GIXRD gave no insight about the morphology of the thin films, we moved to atomic force microscopy (AFM) which gave some insight for the thin film surface morphology. For thin films of polymer **7a** – **9a**, the films are very smooth with rms surface roughness less than 1 nm observed, while only for polymer **6a**, the film is slightly rougher with surface roughness of 2.08 nm (supporting information). For polymer **6a,** the thin film contains multiple elongated features of ~50 - 60nm, which may be due to short-range ordering of isotactic chains, while for atactic polymer **9a**, the film contains multiple isolated circular monticules of 30nm in height, which can be agglomerations of atactic chains.

Similar topology images are obtained in literature for PVK thin films.[52] For polymers **7a** and **8a**, the thin film morphology doesn't have any prominent features.

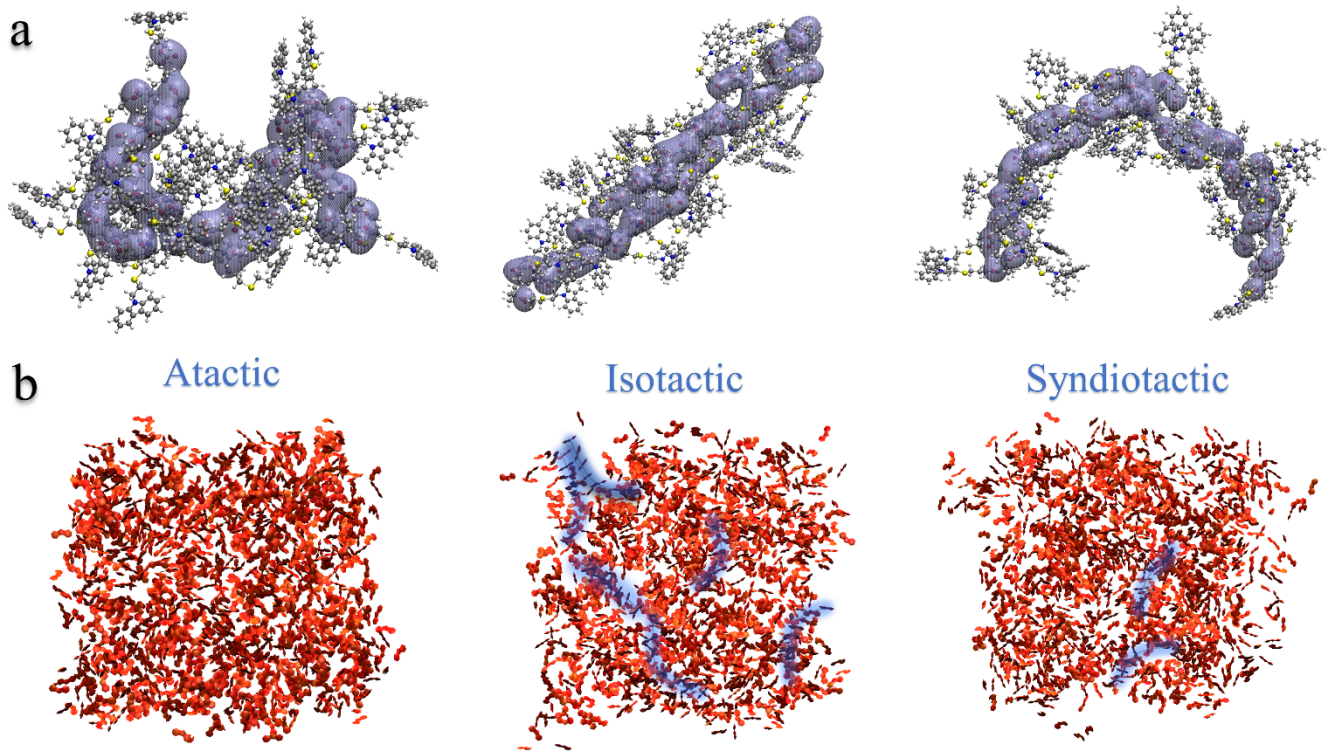

Figure 4. (a) DFT – optimized structures of PCzETPMA polymers with 40 repeating units and highlighted polymer backbone. **(b)** Mapping of carbazole moieties from MD simulated thin films of 64 chains showing short range ordering (blue labelling).

To gain further insight, we elected to turn to simulations to model chain and bulk structures. We used a similar approach as in our previous study[29] using DFT (supporting information). The chains of polymers (atactic, isotactic and syndiotactic) were optimized by using B3LYP/6-31+G in Q-Chem 5.2.[53] From the DFT – optimized structures with 40 repeating units, there is a significant difference between the polymers (Figure **4a**). The atactic structure is more randomized and clumped with respect to the isotactic and syndiotactic structures. In contrast, the isotactic polymer shows an elongated structure but with disordered backbone. On the other hand, the syndiotactic polymer exhibits a curved helical backbone. This type of super helical structure is well known in syndiotactic PMMA polymers.[54] While the atactic polymer shows no $\pi - \pi$ stacking with disorganized pendant units, the isotactic polymer shows some $\pi - \pi$ stacked dimers and trimers within the polymer chain. Interestingly such $\pi - \pi$ stacked trimers were missing in the syndiotactic polymer and are limited to few $\pi - \pi$ stacked dimers.

To understand the effect of annealing and to see how the polymer packs in a thin film, we moved to MD simulations (supporting information). From these MD simulations, we observed that as the films were annealed, the interactions between the chains are enhanced in the case of isotactic and syndiotactic polymers. Upon mapping the carbazole moieties (Figure **4b**), we see short range $\pi - \pi$ stacked ordering between multiple chains in the case of isotactic and syndiotactic polymers, whereas such ordering is absent in the atactic polymer and is limited to $\pi - \pi$ stacked dimers and trimers. Such limited $\pi - \pi$ stacking in the atactic polymer explains the low μ_h observed for polymer **9a**. Although both isotactic and syndiotactic polymers show $\pi - \pi$ stacked short range ordering between multiple chains (not all instances are highlighted in figure **4b**), the isotactic polymer clearly shows more enhanced $\pi - \pi$ stacked arrangements than the syndiotactic counterpart, which explains polymer **6a** having μ_h two orders of magnitude higher than polymer **8a**. All MD simulations were done for 20 repeating units and hence, don't provide any insight for the high molecular weight syndiotactic polymer **7a**. More intensive studies are required for the high molecular weight syndiotactic polymer to understand the dramatic increase in the charge carrier mobility.

Here we have reported the effect of tacticity, annealing and molecular weight in NCPEPs on the charge carrier mobility using PCzETPMA as a model polymer. Specifically, this is the first report of charge carrier mobilities in syndiotactic NCPEPs. The isotactic polymer gave the most consistent charge carrier mobility comparable with conjugated polymers. While a low molecular weight syndiotactic polymer gave similar charge carrier mobility to the atactic counterpart, a high molecular weight syndiotactic polymer gave an unprecedented result surpassing P3HT by an order of magnitude. It is found that enhanced charge carrier mobility in the isotactic polymer is likely due to interchain short range ordering found in thin films as simulated via MD and we suspect that the unprecedented high charge carrier mobility in the high molecular weight syndiotactic polymer is also due to interchain short range ordering, but further experiments are needed to confirm this. These results show that in NCPEPs, tacticity, spacer length and molecular weight are not independent and show a complex relationship, which in some cases leads to charge carrier mobilities exceeding well known conjugated polymers.

ASSOCIATED CONTENT

Supporting Information.

Syntheses of polymers; ^{1}H and ^{13}C spectra; DSC, TGA, CV traces, Charge carrier mobilities (J-V) plots, XRD, AFM and Absorption profiles. DFT and MD simulations of polymers. This material is available free of charge via the Internet at http://pubs.acs.org.

AUTHOR INFORMATION

Corresponding Author

* E-mail: barrycth@usc.edu

Notes

The authors declare no competing financial interest.

ACKNOWLEDGMENT

We acknowledge funding from NSF (CHE-2106405). S.S. also acknowledge funding from USC Dornsife (Stauffer Endowed Fellowship 2020 Award). We acknowledge Dr. Marco Olguin for his insight and help in troubleshooting syntax errors for molecular dynamics calculations. We also acknowledge Prof. Jahan M. Dawalaty for use of their 300 nm UV LED lamp. Finally, we acknowledge Prof. Mark E. Thompson for use of AFM and evaporator.

REFERENCES

(1) Zhan, L.; Li, S.; Xia, X.; Li, Y.; Lu, X.; Zuo, L.; Shi, M.; Chen, H. Layer-by-Layer Processed Ternary Organic Photovoltaics with Efficiency over 18%. *Adv. Mater.* **2021**, *33* (12), 1–9. https://doi.org/10.1002/adma.202007231.

(2) Zhang, M.; Zhu, L.; Zhou, G.; Hao, T.; Qiu, C.; Zhao, Z.; Hu, Q.; Larson, B. W.; Zhu, H.; Ma, Z.; Tang, Z.; Feng, W.; Zhang, Y.; Russell, T. P.; Liu, F. Single-Layered Organic Photovoltaics with Double Cascading Charge Transport Pathways: 18% Efficiencies. *Nat. Commun.* **2021**, *12* (1), 1–10. https://doi.org/10.1038/s41467-020-20580-8.

(3) Li, C.; Zhou, J.; Song, J.; Xu, J.; Zhang, H.; Zhang, X.; Guo, J.; Zhu, L.; Wei, D.; Han, G.; Min, J.; Zhang, Y.; Xie, Z.; Yi, Y.; Yan, H.; Gao, F.; Liu, F.; Sun, Y. Non-Fullerene Acceptors with Branched Side Chains and Improved Molecular Packing to Exceed 18% Efficiency in Organic Solar Cells. *Nat. Energy* **2021**, *6* (6), 605–613. https://doi.org/10.1038/s41560-021-00820-x.

(4) Kim, M.; Ryu, S. U.; Park, S. A.; Choi, K.; Kim, T.; Chung, D.; Park, T. Donor–Acceptor-Conjugated Polymer for High-Performance Organic Field-Effect Transistors: A Progress Report. *Adv. Funct. Mater.* **2020**, *30* (20), 1–25. https://doi.org/10.1002/adfm.201904545.

(5) Lee, H.; Moon, B.; Son, S. Y.; Park, T.; Kang, B.; Cho, K. Charge Trapping in a Low-Crystalline High-Mobility Conjugated Polymer and Its Effects on the Operational Stability of Organic Field-Effect Transistors. *ACS Appl. Mater. Interfaces* **2021**, *13* (14), 16722–16731. https://doi.org/10.1021/acsami.0c20965.

(6) Kang, H. S.; Kim, D. H.; Kim, T. W. Organic Light-Emitting Devices Based on Conducting Polymer Treated with Benzoic Acid. *Sci. Rep.* **2021**, *11* (1), 1–9. https://doi.org/10.1038/s41598-021-82980-0.

(7) Kim, J. H.; Park, J. W. Intrinsically Stretchable Organic Light-Emitting Diodes. *Sci. Adv.* **2021**, *7* (9), 1–11. https://doi.org/10.1126/sciadv.abd9715.

(8) Strietzel, C.; Oka, K.; Strømme, M.; Emanuelsson, R.; Sjödin, M. An Alternative to Carbon Additives: The Fabrication of Conductive Layers Enabled by Soluble Conducting Polymer Precursors - A Case Study for Organic Batteries. *ACS Appl. Mater. Interfaces* **2021**, *13* (4), 5349–5356. https://doi.org/10.1021/acsami.0c22578.

(9) Das, P.; Zayat, B.; Wei, Q.; Salamat, C. Z.; Magdău, I.-B.; Elizalde-Segovia, R.; Rawlings, D.; Lee, D.; Pace, G.; Irshad, A.; Ye, L.; Schmitt, A.; Segalman, R. A.; Miller, T. F.; Tolbert, S. H.; Dunn, B. S.; Narayan, S. R.; Thompson, B. C. Dihexyl-Substituted Poly(3,4-Propylenedioxythiophene) as a Dual Ionic and Electronic Conductive Cathode Binder for Lithium-Ion Batteries. *Chem. Mater.* **2020**, *32* (21), 9176–9189. https://doi.org/10.1021/acs.chemmater.0c02601.

(10) Xu, N.; Mei, S.; Chen, Z.; Dong, Y.; Li, W.; Zhang, C. High-Performance Li-Organic Battery Based on Thiophene-Containing Porous Organic Polymers with Different Morphology and Surface Area as the Anode Materials. *Chem. Eng. J.* **2020**, *395* (January), 124975. https://doi.org/10.1016/j.cej.2020.124975.

(11) Zhang, P.; Travas-Sejdic, J. Fabrication of Conducting Polymer Microelectrodes and Microstructures for Bioelectronics. *J. Mater. Chem. C* **2021**. https://doi.org/10.1039/D1TC01618K.

(12) Higgins, S. G.; Lo Fiego, A.; Patrick, I.; Creamer, A.; Stevens, M. M. Organic Bioelectronics: Using Highly Conjugated Polymers to Interface with Biomolecules, Cells, and Tissues in the Human Body. *Adv. Mater. Technol.* **2020**, *5* (11), 1–35. https://doi.org/10.1002/admt.202000384.

(13) Li, J.; Liang, Z.; Wang, Y.; Li, H.; Tong, J.; Bao, X.; Xia, Y. Enhanced Efficiency of Polymer Solar Cells through Synergistic Optimization of Mobility and Tuning Donor Alloys by Adding High-Mobility Conjugated Polymers. *J. Mater. Chem. C* **2018**, *6* (41), 11015–11022. https://doi.org/10.1039/C8TC03612H.

(14) Qiu, Z.; Hammer, B. A. G.; Müllen, K. Conjugated Polymers – Problems and Promises. *Prog. Polym. Sci.* **2020**, *100*. https://doi.org/10.1016/j.progpolymsci.2019.101179.

(15) Yamashita, Y.; Jhulki, S.; Bhardwaj, D.; Longhi, E.; Kumagai, S.; Watanabe, S.; Barlow, S.; Marder, S. R.; Takeya, J. Highly Air-Stable, n-Doped Conjugated Polymers Achieved by Dimeric Organometallic Dopants. *J. Mater. Chem. C* **2021**, *9* (12), 4105–4111. https://doi.org/10.1039/d0tc05931e.

(16) Chen, A. X.; Kleinschmidt, A. T.; Choudhary, K.; Lipomi, D. J. Beyond Stretchability: Strength, Toughness, and Elastic Range in Semiconducting Polymers. *Chem. Mater.* **2020**, *32* (18), 7582–7601. https://doi.org/10.1021/acs.chemmater.0c03019.

(17) Gobalasingham, N. S.; Carlé, J. E.; Krebs, F. C.; Thompson, B. C.; Bundgaard, E.; Helgesen, M. Conjugated Polymers Via Direct Arylation Polymerization in Continuous Flow: Minimizing the Cost and Batch-to-Batch Variations for High-Throughput Energy Conversion. *Macromol. Rapid Commun.* **2017**, *38* (22), 1700526. https://doi.org/10.1002/marc.201700526.

(18) Pei, D.; Wang, Z.; Peng, Z.; Zhang, J.; Deng, Y.; Han, Y.; Ye, L.; Geng, Y. Impact of Molecular Weight on the Mechanical and Electrical Properties of a High-Mobility Diketopyrrolopyrrole-Based Conjugated Polymer. *Macromolecules* **2020**, *53* (11), 4490–4500. https://doi.org/10.1021/acs.macromol.0c00209.

(19) Xiao, L. L.; Zhou, X.; Yue, K.; Guo, Z. H. Synthesis and Self-Assembly of Conjugated Block Copolymers. *Polymers (Basel).* **2021**, *13* (1), 1–20. https://doi.org/10.3390/polym13010110.

(20) Feng, H.; Lu, X.; Wang, W.; Kang, N.-G.; Mays, J. Block Copolymers: Synthesis, Self-Assembly, and Applications. *Polymers (Basel).* **2017**, *9* (12), 494. https://doi.org/10.3390/polym9100494.

(21) Nikolka, M.; Nasrallah, I.; Rose, B.; Ravva, M. K.; Broch, K.; Sadhanala, A.; Harkin, D.; Charmet, J.; Hurhangee, M.; Brown, A.; Illig, S.; Too, P.; Jongman, J.; McCulloch, I.; Bredas, J. L.; Sirringhaus, H. High Operational and Environmental Stability of High-Mobility Conjugated Polymer Field-Effect Transistors through the Use of Molecular Additives. *Nat. Mater.* **2017**, *16* (3), 356–362. https://doi.org/10.1038/nmat4785.

(22) Wang, M.; Baek, P.; Akbarinejad, A.; Barker, D.; Travas-Sejdic, J. Conjugated Polymers and Composites for Stretchable Organic Electronics. *J. Mater. Chem. C* **2019**, *7* (19), 5534–5552. https://doi.org/10.1039/c9tc00709a.

(23) Lai, W. F. Non-Conjugated Polymers with Intrinsic Luminescence for Drug Delivery. *J. Drug Deliv. Sci. Technol.* **2020**, *59* (April), 101916. https://doi.org/10.1016/j.jddst.2020.101916.

(24) Zhang, Z.; Zhang, Z.; Yu, Y.; Zhao, B.; Li, S.; Zhang, J.; Tan, S. Non-Conjugated Polymers as Thickness-Insensitive Electron Transport Materials in High-Performance Inverted Organic Solar Cells. *J. Energy Chem.* **2020**, *47*, 196–202. https://doi.org/10.1016/j.jechem.2019.12.011.

(25) Lu, Y.; Lin, J.; Wang, L.; Zhang, L.; Cai, C. Self-Assembly of Copolymer Micelles: Higher-Level Assembly for Constructing Hierarchical Structure. *Chem. Rev.* **2020**, *120* (9), 4111–4140. https://doi.org/10.1021/acs.chemrev.9b00774.

(26) Ganicz, T.; Stańczyk, W. *Side-Chain Liquid Crystal Polymers (SCLCP): Methods and Materials. An Overview*; 2009; Vol. 2. https://doi.org/10.3390/ma2010095.

(27) Ndaya, D.; Bosire, R.; Vaidya, S.; Kasi, R. M. Molecular Engineering of Stimuli-Responsive, Functional, Side-Chain Liquid Crystalline Copolymers: Synthesis, Properties and Applications. *Polym. Chem.* **2020**, *11* (37), 5937–5954. https://doi.org/10.1039/D0PY00749H.

(28) Samal, S.; Thompson, B. C. Converging the Hole Mobility of Poly(2- N-Carbazoylethyl Acrylate) with Conjugated Polymers by Tuning Isotacticity. *ACS Macro Lett.* **2018**, *7* (10), 1161–1167. https://doi.org/10.1021/acsmacrolett.8b00595.

(29) Samal, S.; Thompson, B. C. Influence of Alkyl Chain Spacer Length on the Charge Carrier Mobility of Isotactic Poly(N -Carbazolylalkyl Acrylates). *ACS Macro Lett.* **2021**, *10* (6), 720–726. https://doi.org/10.1021/acsmacrolett.1c00249.

(30) Xu, Y.; Bu, T.; Li, M.; Qin, T.; Yin, C.; Wang, N.; Li, R.; Zhong, J.; Li, H.; Peng, Y.; Wang, J.; Xie, L.; Huang, W. Non-Conjugated Polymer as an Efficient Dopant-Free Hole-Transporting Material for Perovskite Solar Cells. *ChemSusChem* **2017**, *10* (12), 2578–2584. https://doi.org/10.1002/cssc.201700584.

(31) Gu, J.; Ji, R.; Xu, W.; Yin, C.; Wen, K.; Gao, H.; Yang, R.; Pan, Z.; Wang, K.; Zhang, C.; Li, R.; Lin, J.; Xie, L.; Wang, J.; Huang, W. Non-Conjugated Polymer Based on Polyethylene Backbone as Dopant-Free Hole-Transporting Material for Efficient and Stable Inverted Quasi-2D Perovskite Solar Cells. *Sol. RRL* **2020**, *4* (7), 2000184. https://doi.org/10.1002/solr.202000184.

(32) D'Angelo, P.; Barra, M.; Cassinese, A.; Maglione, M. G.; Vacca, P.; Minarini, C.; Rubino, A. Electrical Transport Properties Characterization of PVK (Poly N-Vinylcarbazole) for Electroluminescent Devices Applications. *Solid. State. Electron.* **2007**, *51* (1), 101–107. https://doi.org/10.1016/j.sse.2006.11.008.

(33) Uryu, T.; Ohkawa, H.; Oshima, R. Synthesis and High Hole Mobility of Isotactic Poly(2-N-Carbazolylethyl Acrylate). *Macromolecules* **1987**, *20* (4), 712–716. https://doi.org/10.1021/ma00170a002.

(34) Samal, S.; Thompson, B. C. Converging the Hole Mobility of Poly(2- *N*-Carbazoylethyl Acrylate) with Conjugated Polymers by Tuning Isotacticity. *ACS Macro Lett.* **2018**, 1161–1167. https://doi.org/10.1021/acsmacrolett.8b00595.

(35) Kim, W.; Nishikawa, Y.; Watanabe, H.; Kanazawa, A.; Aoshima, S.; Fujii, A.; Ozaki, M. Stereoregularity Effect on Hole Mobility in Poly(N-Vinylcarbazole) Thin Film Evaluated by MIS-CELIV Method. *Jpn. J. Appl. Phys.* **2020**, *59* (SD). https://doi.org/10.7567/1347-4065/ab554f.

(36) Romulus, J.; Henssler, J. T.; Weck, M. Postpolymerization Modification of Block Copolymers. *Macromolecules*. August 26, 2014, pp 5437–5449. https://doi.org/10.1021/ma5009918.

(37) Goldmann, A. S.; Glassner, M.; Inglis, A. J.; Barner-Kowollik, C. Post-Functionalization of Polymers via Orthogonal Ligation Chemistry. In *Chemistry of Organo-Hybrids*; John Wiley & Sons, Inc.: Hoboken, NJ, USA, 2015; pp 395–465. https://doi.org/10.1002/9781118870068.ch11.

(38) Zhang, H.; Ruckenstein, E. Preparation of Functional Polymers by Living Anionic Polymerization: Polymerization of Allyl Methacrylate. *J. Polym. Sci. Part A Polym. Chem.* **1997**, *35* (14), 2901–2906. https://doi.org/10.1002/(SICI)1099-0518(199710)35:14<2901::AID-POLA10>3.0.CO;2-N.

(39) Wiles, D. M.; Brownstein, S. Tacticity Determinations on Allyl Methacrylate Polymers. *J. Polym. Sci. Part B Polym. Lett.* **1965**, *3* (11), 951–954. https://doi.org/10.1002/pol.1965.110031113.

(40) Liras, M.; García-García, J. M.; Quijada-Garrido, I.; Gallardo, A.; París, R. Thermo-Responsive Allyl-Functionalized 2-(2-Methoxyethoxy)Ethyl Methacrylate-Based Polymers as Versatile Precursors for Smart Polymer Conjugates and Conetworks. *Macromolecules* **2011**, *44* (10), 3739–3745. https://doi.org/10.1021/ma200456c.

(41) Xu, J.; Boyer, C. Visible Light Photocatalytic Thiol-Ene Reaction: An Elegant Approach for Fast Polymer Postfunctionalization and Step-Growth Polymerization. *Macromolecules* **2015**, *48* (3), 520–529. https://doi.org/10.1021/ma502460t.

(42) Uryu, T.; Ohaku, K.-I.; Matsuzaki, K. Stereoregularity of Poly(Alkyl α-Chloroacrylates) and Mechanism of Isotactic Polymerization. *J. Polym. Sci. Polym. Chem. Ed.* **1974**, *12* (8), 1723–1734. https://doi.org/10.1002/pol.1974.170120812.

(43) Glusker, D. L.; Galluccio, R. A.; Evans, R. A. The Mechanism of the Anionic Polymerization of Methyl Methacrylate. III. Effects of Solvents upon Stereoregularity and Rates in Fluorenyllithium-Initiated Polymerizations. *J. Am. Chem. Soc.* **1964**, *86* (2), 187–196. https://doi.org/10.1021/ja01056a017.

(44) Fowells, W.; Schuerch, C.; Bovey, F. A.; Hood, F. P. Solvation Control in the Anionic Polymerization of Stereospecifically Deuterated Acrylate and Methacrylate Esters. *J. Am. Chem. Soc.* **1967**, *89* (6), 1396–1404. https://doi.org/10.1021/ja00982a022.

(45) Valade, D.; Boyer, C.; Davis, T. P.; Bulmus, V. Synthesis of SiRNA Polyplexes Adopting a Combination of RAFT Polymerization and Thiol-Ene Chemistry. *Aust. J. Chem.* **2009**, *62* (10), 1344. https://doi.org/10.1071/CH09208.

(46) Brar, A. .; Singh, G.; Shankar, R. Structural Investigations of Poly(Methyl Methacrylate) by Two-Dimensional NMR. *J. Mol. Struct.* **2004**, *703* (1–3), 69–81. https://doi.org/10.1016/j.molstruc.2004.05.030.

(47) Sinha, A. K.; Equbal, D. Thiol–Ene Reaction: Synthetic Aspects and Mechanistic Studies of an Anti-Markovnikov-Selective Hydrothiolation of Olefins. *Asian J. Org. Chem.* **2019**, *8* (1), 32–47. https://doi.org/10.1002/ajoc.201800639.

(48) Roy, D.; Ghosn, B.; Song, E. H.; Ratner, D. M.; Stayton, P. S. Polymer-Trimannoside Conjugates via a Combination of RAFT and Thiol-Ene Chemistry. *Polym. Chem.* **2013**, *4* (4), 1153–1160. https://doi.org/10.1039/c2py20820b.

(49) Kumary, K. L. U.; Pratheek, M.; Hameed, T. A. S.; Predeep, P. Measurement of Hole Mobility in P3HT Based Photovoltaic Cell Using Space Charge Limited Current Method. In *AIP Conference Proceedings*; 2019; Vol. 2162, p 020142. https://doi.org/10.1063/1.5130352.

(50) Martins, T. D.; Weiss, R. G.; Atvars, T. D. Z. Synthesis and Photophysical Properties of a Poly(Methyl Methacrylate) Polymer with Carbazolyl Side Groups. *J. Braz. Chem. Soc.* **2008**, *19* (8), 1450–1461. https://doi.org/10.1590/S0103-50532008000800003.

(51) Talik, N. A.; Yap, B. K.; Tan, C. Y.; Whitcher, T. J. In-Situ Analysis Energy Level Alignment at Solution Processed HAT(CN)6/PVK (PVK:TAPC) Interface via XPS and UPS. *Curr. Appl. Phys.* **2017**, *17* (8), 1094–1099. https://doi.org/10.1016/j.cap.2017.04.012.

(52) Shao, Y.; Gan, Z.; Epifanovsky, E.; Gilbert, A. T. B.; Wormit, M.; Kussmann, J.; Lange, A. W.; Behn, A.; Deng, J.; Feng, X.; Ghosh, D.; Goldey, M.; Horn, P. R.; Jacobson, L. D.; Kaliman, I.; Khaliullin, R. Z.; Kuś, T.; Landau, A.; Liu, J.; Proynov, E. I.; Rhee, Y. M.; Richard, R. M.; Rohrdanz, M. A.; Steele, R. P.; Sundstrom, E. J.; Woodcock, H. L.; Zimmerman, P. M.; Zuev, D.; Albrecht, B.; Alguire, E.; Austin, B.; Beran, G. J. O.; Bernard, Y. A.; Berquist, E.; Brandhorst, K.; Bravaya, K. B.; Brown, S. T.; Casanova, D.; Chang, C.-M.; Chen, Y.; Chien, S. H.; Closser, K. D.; Crittenden, D. L.; Diedenhofen, M.; DiStasio, R. A.; Do, H.; Dutoi, A. D.; Edgar, R. G.; Fatehi, S.; Fusti-Molnar, L.; Ghysels, A.; Golubeva-Zadorozhnaya, A.; Gomes, J.; Hanson-Heine, M. W. D.; Harbach, P. H. P.; Hauser, A. W.; Hohenstein, E. G.; Holden, Z. C.; Jagau, T.-C.; Ji, H.; Kaduk, B.; Khistyaev, K.; Kim, J.; Kim, J.; King, R. A.; Klunzinger, P.; Kosenkov, D.; Kowalczyk, T.; Krauter, C. M.; Lao, K. U.; Laurent, A. D.; Lawler, K. V.; Levchenko, S. V.; Lin, C. Y.; Liu, F.; Livshits, E.; Lochan, R. C.; Luenser, A.; Manohar, P.; Manzer, S. F.; Mao, S.-P.; Mardirossian, N.; Marenich, A. V.; Maurer, S. A.; Mayhall, N. J.; Neuscamman, E.; Oana, C. M.; Olivares-Amaya, R.; O'Neill, D. P.; Parkhill, J. A.; Perrine, T. M.; Peverati, R.; Prociuk, A.; Rehn, D. R.; Rosta, E.; Russ, N. J.; Sharada, S. M.; Sharma, S.; Small, D. W.; Sodt, A.; Stein, T.; Stück, D.; Su, Y.-C.; Thom, A. J. W.; Tsuchimochi, T.; Vanovschi, V.; Vogt, L.; Vydrov, O.; Wang, T.; Watson, M. A.; Wenzel, J.; White, A.; Williams, C. F.; Yang, J.; Yeganeh, S.; Yost, S. R.; You, Z.-Q.; Zhang, I. Y.; Zhang, X.; Zhao, Y.; Brooks, B. R.; Chan, G. K. L.; Chipman, D. M.; Cramer, C. J.; Goddard, W. A.; Gordon, M. S.; Hehre, W. J.; Klamt, A.; Schaefer, H. F.; Schmidt, M. W.; Sherrill, C. D.; Truhlar, D. G.; Warshel, A.; Xu, X.; Aspuru-Guzik, A.; Baer, R.; Bell, A. T.; Besley, N. A.; Chai, J.-D.; Dreuw, A.; Dunietz, B. D.; Furlani, T. R.; Gwaltney, S. R.; Hsu, C.-P.; Jung, Y.; Kong, J.; Lambrecht, D. S.; Liang, W.; Ochsenfeld, C.; Rassolov, V. A.; Slipchenko, L. V.; Subotnik, J. E.; Van Voorhis, T.; Herbert, J. M.; Krylov, A. I.; Gill, P. M. W.; Head-Gordon, M. Advances in Molecular Quantum Chemistry Contained in the Q-Chem 4 Program Package. *Mol. Phys.* **2015**, *113* (2), 184–215. https://doi.org/10.1080/00268976.2014.952696.

(53) Christofferson, A. J.; Yiapanis, G.; Ren, J. M.; Qiao, G. G.; Satoh, K.; Kamigaito, M.; Yarovsky, I. Molecular Mapping of Poly(Methyl Methacrylate) Super-Helix Stereocomplexes. *Chem. Sci.* **2015**, *6* (2), 1370–1378. https://doi.org/10.1039/c4sc02971b.

Insert Table of Contents artwork here